Proceedings of the 17th World Congress
The International Federation of Automatic Control
Seoul, Korea, July 6-11, 2008

Set membership estimation of fractional models in the frequency domain

F. Khemane, R. Malti, M. Thomassin, and T. Raïssi

IMS, UMR 5218 CNRS, Université Bordeaux 1, 351 cours de la Libération, F 33405 Talence cedex, France – e-mail: {firas.khemane, rachid.malti, magalie.thomassin, tarek.raissi}@laps.ims-bordeaux.fr

Abstract: The main objective of this paper is to estimate the whole set of feasible parameters of a fractional differentiation model, based on gain and phase frequency data. All parameters, including differentiation orders, are expressed as intervals and then estimated using a bounded error approach. A contraction method named *forward-backward propagation* is first applied to reduce the initial searching space. Then, a set inversion algorithm named *SIVIA* is applied on the reduced searching space to obtain the whole set of feasible parameters. One of the interesting points of this study is to show the separate contribution of gain and phase data on the final estimation.

Keywords: Fractional models; Bounded error; System identification; Frequency-domain data; Gain; Phase.

1. INTRODUCTION AND MATHEMATICAL BACKGROUND

Although fractional (non integer) integration and differentiation remained for a long time purely a mathematical concept, the last two decades have witnessed considerable development in the use of fractional operators in various fields. Fractional differentiation is now an important tool for the international scientific and industrial communities especially in modeling viscoelastic materials (Pritz (2003)) and some diffusive phenomena (thermal diffusion, electrochemical diffusion) or in financial systems (Chen (2008)). For example, in thermal diffusion in a semi-infinite homogeneous medium, Battaglia et al. (2001) have shown that the exact solution for the heat equation links the thermal flux to a half order derivative of the surface temperature on which the flux is applied. Diffusion phenomena were investigated in semi-infinite planar, spherical and cylindrical media by Oldham and Spanier (1972, 1973) who showed that the involved transfer functions use the Laplace variable s with exponents multiples of 0.5. In electrochemical diffusion of charges in the electrode and the electrolyte, the most common physical model used in the litterature is the Randles model (Rodrigues et al. (2000); Sabatier et al. (2006)) which uses Warburg impedance with an integrator of order 0.5. Frequency domain response of fractional models is characterized by the presence of any slope in Bode's gain diagram and any phase lock in Bode's phase diagram.

Frequency-domain system identification methods using fractional models was initiated by Mathieu et al. (1995); Le Lay (1998); as detailed in the tutorial paper Malti et al. (2006). Recently Valério and da Costa (2007) extended Levy's identification technics (Levy (1959)), and its improvements by Sanathanan and Koerner (1963) and by Lawrence and Rogers (1979), to deal with fractional models. Most of the proposed identification methods are based on the minimization of the (weighted or not) ℓ_2-norm of the fitting error. All these methods use prior knowledge to fix differentiation orders. Optimizing differentiation orders is more complex as the model is non linear with respect to these parameters. The quadratic criterion could be non convex and gradient-based algorithm could fail in finding the global minimum, if the algorithm is initialized in the vicinity of a local one.

The objective of this paper is to estimate the whole set of feasible parameters of a fractional differentiation model, based on frequency domain uncertain but bounded data.

1.1 Fractional models

A fractional mathematical model is based on a fractional differential equation:

$$y(t) + a_1 \mathbf{D}^{\alpha_1} y(t) + \cdots + a_{m_A} \mathbf{D}^{\alpha_{m_A}} y(t) = b_0 \mathbf{D}^{\beta_0} u(t) + b_1 \mathbf{D}^{\beta_1} u(t) + \cdots + b_{m_B} \mathbf{D}^{\beta_{m_B}} u(t), \quad (1)$$

where $(a_i, b_j) \in \mathbb{R}^2$, differentiation orders $\alpha_1 < \alpha_2 < \ldots < \alpha_{m_A}$, $\beta_0 < \beta_1 < \ldots < \beta_{m_B}$ are allowed to be non-integer positive numbers. The concept of differentiation to an arbitrary order,

$$\mathbf{D}^{\nu} \triangleq \left(\frac{d}{dt}\right)^{\nu}, \qquad \forall \nu \in \mathbb{R}_{+}^{*}, \quad (2)$$

was defined in the 19$^{\text{th}}$ century by Riemann and Liouville. The ν fractional derivative of $x(t)$ is defined as being an integer derivative of order $\lfloor \nu \rfloor + 1$ ($\lfloor . \rfloor$ stands for the floor operator) of a non-integer integral of order $\lfloor \nu \rfloor + 1 - \nu$ (Samko et al. (1993)):

$$\mathbf{D}^{\nu} x(t) = \mathbf{D}^{\lfloor \nu \rfloor + 1}\left(\mathbf{I}^{\lfloor \nu \rfloor + 1 - \nu} x(t)\right) \triangleq \left(\frac{d}{dt}\right)^{\lfloor \nu \rfloor + 1}\left(\frac{1}{\Gamma(\lfloor \nu \rfloor + 1 - \nu)} \int_0^t \frac{x(\tau)\, d\tau}{(t-\tau)^{\nu - \lfloor \nu \rfloor}}\right), \quad (3)$$

where $t > 0, \forall \nu \in \mathbb{R}_+^*$, and the Euler's Γ function is defined for a complex number z with positive real part by:

$$\Gamma(z) = \int_0^\infty t^{z-1} e^{-t} dt, \tag{4}$$

which can be extended, by analytical continuity, to the rest of the complex plane.

The Laplace transform is a more concise algebraic tool generally used to represent fractional systems, (see Oldham and Spanier (1974)):

$$\mathscr{L}\{\mathbf{D}^\nu x(t)\} = s^\nu \mathscr{L}\{x(t)\}, \qquad \text{if } x(t) = 0\ \forall t \leq 0. \tag{5}$$

This property allows to write the fractional differential equation (1), provided $u(t)$ and $y(t)$ are relaxed at $t = 0$, in a transfer function form:

$$F(s) = \frac{\sum_{j=0}^{m_B} b_j s^{\beta_j}}{1 + \sum_{i=1}^{m_A} a_i s^{\alpha_i}}. \tag{6}$$

The function s^ν, where s belongs to the set of complex numbers $\mathbb{C}$, is multivalued as soon as ν is not integer. A branch cut line is defined along the negative real axis $\mathbb{R}_-$ and the function s^ν becomes holomorphic in the complement of the branch cut line, i.e. in $\mathbb{C} \setminus \mathbb{R}_-$. All arguments of s are then restricted to $]-\pi, \pi[$.
A modal form transfer function can then be obtained, by carrying out a partial fraction expansion of (6) on the s^ν variable, provided (6) is strictly proper and commensurable [1] of order ν:

$$F(s) = \sum_{k=1}^{N} \sum_{q=1}^{v_k} \frac{A_{k,q}}{(s^\nu + B_k)^q}, \tag{7}$$

where $(-B_k), k = 1, \ldots, N$ are known as the s^ν-poles of integer multiplicity v_k.

Stability of any fractional commensurable transfer function such as (6) is proved by Matignon (1998) and is presented for any $\nu \in]0, 2[$ in the following theorem.

Theorem 1. A commensurable ν-order transfer function $F(s) = S(s^\nu) = \frac{T(s^\nu)}{R(s^\nu)}$, where T and R are two coprime polynomials, is stable iff $0 < \nu < 2$ and $\forall p \in \mathbb{C}$ such as $R(p) = 0$, $|\arg(p)| > \nu\frac{\pi}{2}$.

The stability region suggested by this theorem tends to the whole s-plane when ν tends to 0, corresponds to the Rooth-Hurwitz stability when $\nu = 1$, and tends to the negative real axis when ν tends to 2.

1.2 Problem formulation

The fractional model considered in this paper is the building block of the modal form (7):

$$G(s) = \frac{K}{s^\nu + b}, \tag{8}$$

where the non integer differentiation order, ν, is restricted to the interval $]0, 2[$ and the pole in s^ν, $-b$, is restricted to the negative real axis in order to guarantee model's stability, as specified by theorem 1, and the realness of the time-domain response of $G(s)$. A complex b would generate a complex impulse response.

[1] All differentiation orders are exactly divisible by the same number (ν) an integral number of times (The American Heritage ® (2000)).

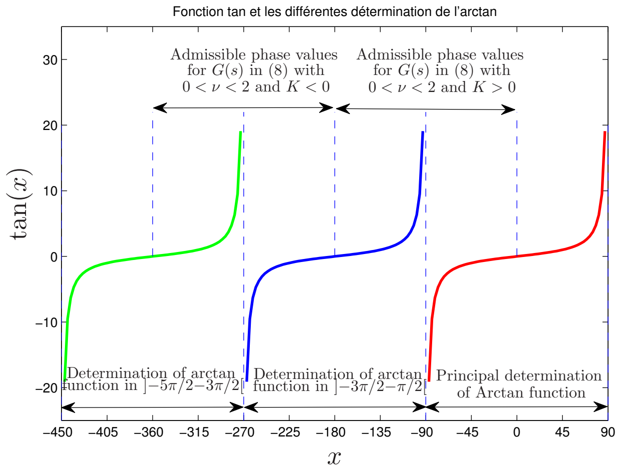

Fig. 1. Admissible phase values of $G(s)$ in (8) for different signs of K and three possible determinations of arctan function.

Frequency domain uncertain data are considered as gain in dB and phase in degrees. Data are supposed to be altered by a bounded noise with an unknown distribution. Such data may be acquired from: (i) frequency analysis of input/output signals, or (ii) bounded non parametric frequency identification methods (Ljung (1999)) using one or multiple experiments. One of the difficulties, not addressed here, is how to convert time-domain uncertainties into frequency domain uncertainties. Some elements allowing to answer this question can be found in (Antoni and Schoukens (2007)).

Frequency gain and phase characteristics of (8) are obtained by replacing s by $j\omega$:

$$G(j\omega) = \frac{K}{(j\omega)^\nu + b}. \tag{9}$$

Since the argument of s is restricted to $]-\pi, \pi[$, j is replaced by $e^{j\frac{\pi}{2}}$:

$$G(j\omega) = \frac{K}{\left(e^{j\frac{\pi}{2}}\omega\right)^\nu + b} = \frac{K}{\left(\cos(\nu\frac{\pi}{2}) + j\sin(\nu\frac{\pi}{2})\right)\omega^\nu + b}. \tag{10}$$

Then, the gain and the phase are obtained by taking the modulus and the argument of (10):

$$\begin{aligned} G_{\mathrm{dB}}(\omega) &= 10\log\left(\frac{K^2}{(b + \cos(\nu\frac{\pi}{2})\omega^\nu)^2 + (\sin(\nu\frac{\pi}{2})\omega^\nu)^2}\right), \\ &= 10\log\left(\frac{K^2}{b^2 + 2b\cos(\nu\frac{\pi}{2})\omega^\nu + \omega^{2\nu}}\right), \end{aligned} \tag{11}$$

$$\varphi(\omega) = \begin{cases} -Arctan\left(\dfrac{\sin(\nu\frac{\pi}{2})\omega^\nu}{\mathrm{Den}(\omega)}\right), & \text{if } \mathrm{Den}(\omega) > 0, \\ -\pi - Arctan\left(\dfrac{\sin\left(\nu\frac{\pi}{2}\right)\omega^\nu}{\mathrm{Den}(\omega)}\right), & \text{if } \mathrm{Den}(\omega) < 0, \end{cases} \tag{12}$$

where $\mathrm{Den}(\omega) = b + \cos\left(\nu\frac{\pi}{2}\right)\omega^\nu$. Eq. (12) is given for $K > 0$ (in case $K < 0, \pi$ is substracted from each equation in (12)). As shown in Fig. 1, when $0 < \nu < 2$, phase admissible values of (8) range from $-180°$ to 0 if $K > 0$ and from $-360°$ to $-180°$ if $K < 0$. Each interval ranges over three determinations of the arctan function.

Hence, **the problem at stake is the following**. Having a set of N bounded uncertain frequency-domain gain and phase data, respectively

$$[G_{\mathrm{dB}}(\omega_i)] = \left[\underline{G_{\mathrm{dB}}}(\omega_i), \overline{G_{\mathrm{dB}}}(\omega_i)\right], \quad (13)$$

$$[\varphi(\omega_i)] = \left[\underline{\varphi}(\omega_i), \overline{\varphi}(\omega_i)\right], \quad (14)$$

where $i = 1, \ldots, N$, **find the set of all feasible parameters of the fractional model (8)**.

A parameter vector $\boldsymbol{\theta} = (K, b, \nu)^T$ is called feasible if the model evaluated with $\boldsymbol{\theta}$ is consistent with the measurements and with the error bounds. The parameter estimation problem is considered as a constraint satisfaction problem ($\mathcal{CSP}$) which is solved using interval analysis, initially introduced by Moore (1966). An interval $[x] = [\underline{x}, \overline{x}]$ is a closed, bounded, and connected set of real numbers. The set of all intervals is denoted by $\mathbb{IR}$. Real operations are extended to intervals as follows. Given $[x] \in \mathbb{IR}$ and $[y] \in \mathbb{IR}$:

$$[x] + [y] = [\underline{x} + \underline{y}, \overline{x} + \overline{y}], \quad (15)$$

$$[x] - [y] = [\underline{x} - \overline{y}, \overline{x} - \underline{y}], \quad (16)$$

$$[x] \times [y] = [\min(\underline{x}\underline{y}, \underline{x}\overline{y}, \overline{x}\underline{y}, \overline{x}\overline{y}), \max(\underline{x}\underline{y}, \underline{x}\overline{y}, \overline{x}\underline{y}, \overline{x}\overline{y})] \quad (17)$$

$$[x]/[y] = \begin{cases} [x] \times \left[\dfrac{1}{\overline{y}}, \dfrac{1}{\underline{y}}\right], & \text{if } 0 \notin [y] \\ ]-\infty, \infty[, & \text{if } 0 \in [y]. \end{cases} \quad (18)$$

2. FORWARD-BACKWARD CONTRACTOR

The $\mathcal{CSP}$ to be solved is given by:

$$\mathcal{CSP}: \begin{cases} \underline{G_{\mathrm{dB}}}(\omega_i) \leq G_{\mathrm{dB}}(\omega_i, \boldsymbol{\theta}) \leq \overline{G_{\mathrm{dB}}}(\omega_i), \\ \underline{\varphi}(\omega_i) \leq \varphi(\omega_i, \boldsymbol{\theta}) \leq \overline{\varphi}(\omega_i), i \in \{1, \ldots, N\}, \\ -\infty < K < \infty, \quad 0 < b < \infty, \quad 0 < \nu < 2, \end{cases} \quad (19)$$

where $\underline{G}(\omega_i)$, $\overline{G}(\omega_i)$, $\underline{\varphi}(\omega_i)$, and $\overline{\varphi}(\omega_i)$ are defined in (13) and (14). Notations $G_{\mathrm{dB}}(\omega_i, \boldsymbol{\theta})$ and $\varphi(\omega_i, \boldsymbol{\theta})$ are used instead of $G_{\mathrm{dB}}(\omega_i)$ and $\varphi(\omega_i)$ to show that (11) and (12) depend on the parameter vector $\boldsymbol{\theta} = (K, b, \nu)^T$. The lower bound of b and the interval of ν are chosen so as to satisfy the stability conditions of theorem 1.

The solution set $\mathbb{S}$ of the $\mathcal{CSP}$ (19) can be rewritten as:

$$\mathbb{S} = \left\{\boldsymbol{\theta} \in \Theta \mid f(\omega_i, \boldsymbol{\theta}) \in [y(\omega_i)], i \in \{1, \ldots, N\}\right\}, \quad (20)$$

where $f = G_{\mathrm{dB}}$ or $f = \varphi$ and $[y(\omega_i)] = [G_{\mathrm{dB}}(\omega_i)]$ or $[y(\omega_i)] = [\varphi(\omega_i)]$. The characterization of the whole set $\mathbb{S}$ can be formulated as a set inversion problem:

$$\mathbb{S} = f^{-1}([y]) \cap \Theta, \quad (21)$$

and can be solved by guaranteed methods.

The $\mathcal{CSP}$ (19) is solved by a contractor $\mathcal{C}$, which is an operator which permits to reduce the domain $[\boldsymbol{\theta}]$ without any bisection. Hence, contracting the box $[\boldsymbol{\theta}]$ means replacing it by a smaller box $[\boldsymbol{\theta}]^*$ such that the solution set $\mathbb{S}$ remains unchanged, i.e. $\mathbb{S} \subset [\boldsymbol{\theta}]^* \subset [\boldsymbol{\theta}]$ (Jaulin et al. (2001)). There exists different types of contractors depending on whether the system to be solved is linear or not.
In our study, a non linear type contractor named *forward-backward contractor* $\mathcal{C}_{\downarrow\uparrow}$ is used to reduce the initial searching space. The basic idea when implementing this contractor is to decompose a principale constraint into primitive constraints. Each primitive constraint involves elementary operators and functions such as $\{+, -, \times, /, \exp, \log \ldots\}$. The next example illustrates how a given constraint is used to contract a domain.

Example Consider the constraint:

$$\begin{cases} f(\mathbf{x}) = x_3 - x_2 x_1 = 0, \\ x_1 \in [2, 10],\ x_2 \in [1, 10],\ x_3 \in [1, 5], \end{cases} \quad (22)$$

The constraint (22) can be rewritten as:

$$x_3 = x_2 x_1.$$

The forward interval constraint propagation will remove all inconsistent values from $[x_3]$ as follows:

$$[x_3] = ([x_1] \times [x_2]) \cap [x_3] = [2, 5].$$

Then, the backward interval constraint propagation will remove all inconsistent values from x_1 and x_2 as follows:

$$[x_1] = ([x_3]/[x_2]) \cap [x_1] = [2, 5],$$
$$[x_2] = ([x_3]/[x_1]) \cap [x_2] = [1, 5/2].$$

After a forward and a backward propagation, the contracted box is $[\mathbf{x}] = \left([2, 5], [1, 5/2], [2, 5]\right)^T$ which contains the solution of the $\mathcal{CSP}$.

As described in this example, in some cases the contractor cannot reduce enough the domain of the parameters. In such a case, the bisection of the variables vector $\mathbf{x}$ is necessary. The algorithm SIVIA (Jaulin and Walter (1993)) which is described in the following section is based on the association of contractors and splitting. It is applied, in this paper, to the gain and the phase constraints (19) following the same stages as described in the previous example.

3. SET INVERSION VIA INTERVAL ANALYSIS (SIVIA)

This algorithm, proposed by Jaulin and Walter (1993), allows to obtain an inner $\underline{\mathbb{S}}$ and an outer $\overline{\mathbb{S}}$ enclosures of the solution set $\mathbb{S}$ (if it exists), such that:

$$\underline{\mathbb{S}} \subseteq \mathbb{S} \subseteq \overline{\mathbb{S}}. \quad (23)$$

SIVIA is a recursive algorithm based on partitioning the parameter set into three regions: feasible, undeterminate and unfeasible. SIVIA uses an inclusion test $[t]$ which is a function allowing to prove if an interval $[\boldsymbol{\theta}]$ is feasible in which case it is added to the set $\underline{\mathbb{S}}$. Any undetermined region is bisected and tested again, unless its size $w([\boldsymbol{\theta}])$ is less than a precision parameter η tuned by the user and which ensures that the algorithm terminates after a finite number of iterations. The outer approximation is then computed as $\overline{\mathbb{S}} = \underline{\mathbb{S}} \cup \Delta\mathbb{S}$ where $\Delta\mathbb{S}$ is the union of all remaining undetermined boxes. Hence, the SIVIA algorithm is presented as follow:

Algorithm SIVIA (in: $[t], [\boldsymbol{\theta}], \eta$; out: $\underline{\mathbb{S}}, \overline{\mathbb{S}}$)

(1) If $[t]([\boldsymbol{\theta}]) = [0]$, return;
(2) If $[t]([\boldsymbol{\theta}]) = [1]$, then $\underline{\mathbb{S}} := \underline{\mathbb{S}} \cup [\boldsymbol{\theta}]; \overline{\mathbb{S}} := \overline{\mathbb{S}} \cup [\boldsymbol{\theta}]$, return;
(3) If $w([\boldsymbol{\theta}]) \leq \eta, \overline{\mathbb{S}} := \overline{\mathbb{S}} \cup [\boldsymbol{\theta}]$;
Else bisecte $[\boldsymbol{\theta}]$ into $[\boldsymbol{\theta}_1]$ and $[\boldsymbol{\theta}_2]$;
(4) SIVIA (in: $[t], [\boldsymbol{\theta}_1], \eta$; out: $\underline{\mathbb{S}}, \overline{\mathbb{S}}$);
(5) SIVIA (in: $[t], [\boldsymbol{\theta}_2], \eta$; out: $\underline{\mathbb{S}}, \overline{\mathbb{S}}$).

4. EXAMPLE

The following transfer function is chosen to generate data:

$$G(s) = \frac{3}{2 + s^{0.5}}. \quad (24)$$

The frequency response of $G(s)$ is obtained by replacing s by $j\omega$:

$$G(j\omega) = \frac{3}{2 + (j\omega)^{0.5}}. \tag{25}$$

Thus, the gain in dB is:

$$G_{\mathrm{dB}}(\omega) = 20 \log \left| \frac{3}{2 + (j\omega)^{0.5}} \right|, \tag{26}$$

and the phase in degrees is:

$$\varphi(\omega) = \arg \left(\frac{3}{2 + (j\omega)^{0.5}} \right). \tag{27}$$

Frequency-domain data are generated by taking 50 log-equidistant frequencies in the range $[10^{-4}, 10^{4}]$ and computing $G_{\mathrm{dB}}(\omega)$ and $\varphi(\omega)$ according to (26) and (27), which are then corrupted by a frequency domain additive noise:

$$G^{\star}_{\mathrm{dB}}(\omega) = G_{\mathrm{dB}}(\omega) + b_{\mathrm{dB}}(\omega), \tag{28}$$

$$\varphi^{\star}(\omega) = \varphi(\omega) + b_{\varphi}(\omega). \tag{29}$$

where the noises $b_{\mathrm{dB}(\omega)}$ and $b_{\varphi}(\omega)$ are generated in the same way:

$$b_{\{\mathrm{dB},\varphi\}}(\omega) = \begin{cases} 1.5\rho_{\{\mathrm{dB},\varphi\}}, & \text{in low freq.,} \\ 1.5\rho_{\{\mathrm{dB},\varphi\}} \times \log(\omega), & \text{in high freq.,} \end{cases} \tag{30}$$

with $\rho_{\{\mathrm{dB},\varphi\}}$ a random variable uniformly distributed between -1 and 1. A higher amplitude noise is added in high frequencies, because time-domain additive noise is generally higher in high frequencies.

For each gain and phase datum, uncertainties are added as intervals of amplitude a bit higher than the worst case noise generated by (30), so that these data can lead to feasible parameters sets with a non-empty inner enclosure $\underline{\mathbb{S}}$:

$$[G^{\star}_{\mathrm{dB}}(\omega)] = G^{\star}_{\mathrm{dB}}(\omega) + \begin{cases} 2 \times [-1, 1], & \text{in low freq.,} \\ 2 \times [-\log(\omega), \log(\omega)], & \text{in high freq.} \end{cases} \tag{31}$$

$$[\varphi^{\star}(\omega)] = \varphi^{\star}(\omega) + \begin{cases} 2 \times [-1, 1], & \text{in low freq.,} \\ 2 \times [-\log(\omega), \log(\omega)], & \text{in high freq.} \end{cases} \tag{32}$$

Fig. 2 shows the frequency uncertain but bounded response obtained according to the previous hypotheses.

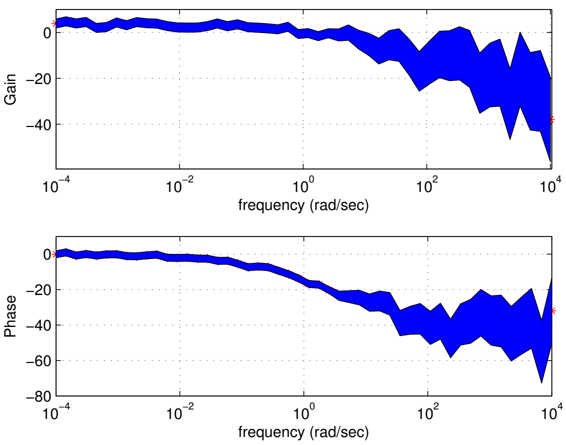

Fig. 2. Uncertain gain and phase data

4.1 Gain and phase contractors

The $\mathcal{CSP}$ to be solved here is given by (19). The initial searching box is set to:

$$\big([K], [b], [\nu]\big) = \big([-20, 20], [0.1, 10], [0.2, 1.9]\big). \tag{33}$$

Let's start by checking how gain and phase data contract separately the initial searching box. The forward-backward contractor $\mathcal{C}_{\downarrow\uparrow}$, explained in §2, is first applied on gain data for every frequency ω_i by decomposing (11) into elementary operations. The main drawback of this operation is the multiple occurrences of the parameters to be estimated, which induce pessimism due to the dependence effect. The following contracted box is obtained:

$$\big([K], [b], [\nu]\big) = \big([-12.67, 12.67], [0.1, 10], [0.2, 1]\big). \tag{34}$$

Since the gain (13) does not depend on the sign of K in (8), positive and negative K's are contracted in the same way. Parameter b was not contracted (Fig. 3).
In the same way, the contractor $\mathcal{C}_{\downarrow\uparrow}$ is applied on phase data (12) taken separately. The following contracted box is obtained:

$$\big([K], [b], [\nu]\big) = \big([0, 20], [0.1, 5.81], [0.2, 1.6]\big). \tag{35}$$

Since the phase (14) depends only on the sign of K in (8), the initial searching domain of $[K]$, *i.e* $[-20, 20]$, is contracted to $[0, 20]$ (Fig. 3).
Following the same method, $\mathcal{C}_{\downarrow\uparrow}$ contractor is applied on phase and gain data simultaneously which yields a smaller contracted box (Fig. 3).

$$\big([K], [b], [\nu]\big) = \big([0, 12.67], [0.1, 4.48], [0.2, 1]\big). \tag{36}$$

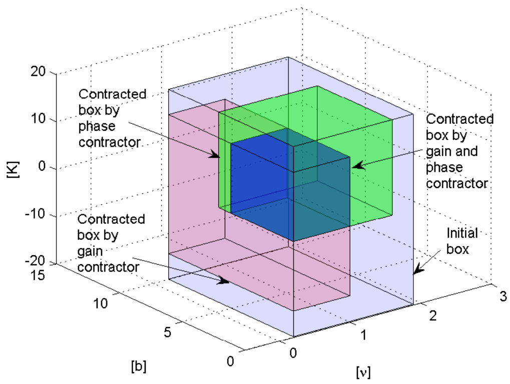

Fig. 3. Initial and contracted boxes by gain and phase contractors.

4.2 Applying SIVIA on gain data

To check the separate contributions of phase and gain data in the final model, SIVIA algorithm is first of all applied on gain data separately and is hence initialized by using the gain contracted box (34). The obtained inner and outer approximations of $[\boldsymbol{\theta}] = ([K], [b], [\nu])^T$ are plotted in Fig. 4. Two disconnected solution sets are obtained. They are symmetrical with respect to $K = 0$, because the gain (11) does not depend on the sign of K in (8). The inner solution sets of $[\boldsymbol{\theta}]$ are enclosed in:

$$\begin{cases} \big([2.07, 4, 43], [1.26, 3.17], [0.34, 0.64]\big) \text{ for } K > 0, \\ \big([-4, 43, -2.07], [1.26, 3.17], [0.34, 0.64]\big) \text{ for } K < 0. \end{cases} \tag{37}$$

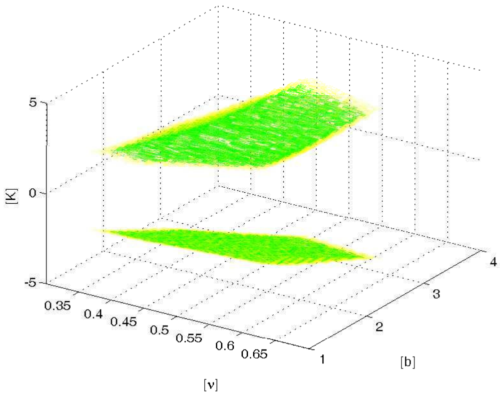

Fig. 4. Inner (dark) and outer (light) solutions obtained for $\eta = 0.01$. Number of bisections 343,503.

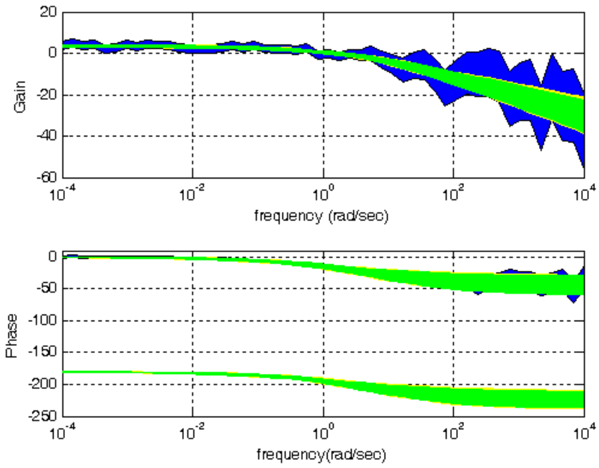

Fig. 5. Gain and phase diagrams of inner (dark) and outer (light) solution sets obtained by applying SIVIA on gain data.

The gain and the phase diagrams of all feasible models obtained here are plotted in Fig. 5. One can notice that guaranteed-models' gain diagrams are all included in the gain uncertainty intervals. However, some models phase diagrams, and especially those generated by negative K's, are outside phase uncertainty intervals. This is a normal fact since only gain data are used as constraints of the set inversion problem.

4.3 Applying SIVIA on phase data

SIVIA algorithm is now applied on phase data separately and is hence initialized by using the phase contracted box (35). Remember that only the sign of K acts on the phase. Hence, phase information can help finding the sign of K and the feasible parameters $[b]$ and $[\nu]$. On the other side, the phase contracted box (35) has already showed that the gain is positive. The obtained inner and outer approximations of $[b]$ and $[\nu]$ are hence plotted in 2D in Fig. 6. The inner solution sets of $[\boldsymbol{\theta}]$ are enclosed in:

$$\big([K],[b],[\nu]\big) = \big([0, 12.34], [1.75, 2.15], [0.47, 0.52]\big). \quad (38)$$

The gain and the phase diagrams of all feasible models obtained here are plotted in Fig. 7. One can notice that

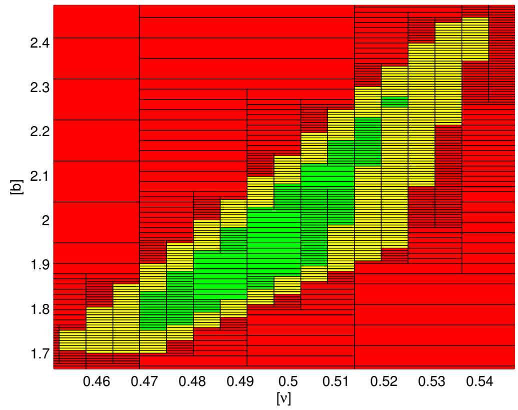

Fig. 6. Inner (dark) and outer (light) solutions obtained for $\eta = 0.01$. Number of bisections 2,549.

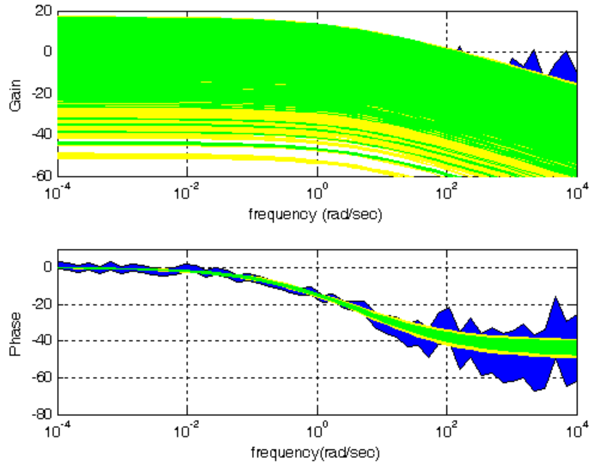

Fig. 7. Gain and phase diagrams of inner (dark) and outer (light) solution sets obtained by applying SIVIA on phase data.

guaranteed-models phase diagrams are all included in the phase uncertainty intervals. However, some models gain diagrams are outside gain uncertainty intervals. This is a normal fact since only phase data are used as constraints of the set inversion problem and any positive gain could fit in.

4.4 Applying SIVIA on gain and phase data simultaneously

SIVIA algorithm is now applied on gain and phase data simultaneously and is hence initialized by using the gain and phase contracted box (36). The obtained inner and outer approximations of $[\boldsymbol{\theta}]$ are plotted in Fig. 8. The inner solution sets are enclosed in:

$$\big([K],[b],[\nu]\big) = \big([2.57, 3.51], [1.76, 2.21], [0.47, 0.52]\big). \quad (39)$$

The gain and the phase diagrams of feasible models are plotted in Fig. 9. Now, feasible gain and phase diagrams are all included in the gain and phase uncertainty intervals. This is a normal fact since both gain and phase data are used in the set inversion problem.

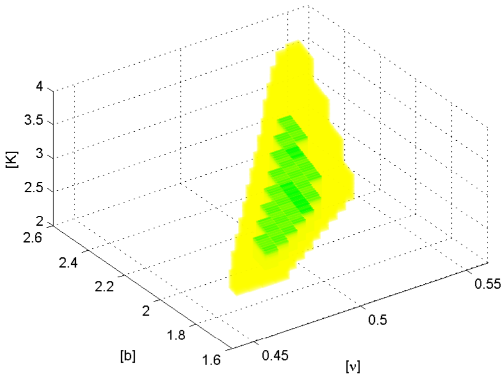

Fig. 8. Inner (dark) and outer (light) solutions obtained for $\eta = 0.01$. Number of bisections 83,245.

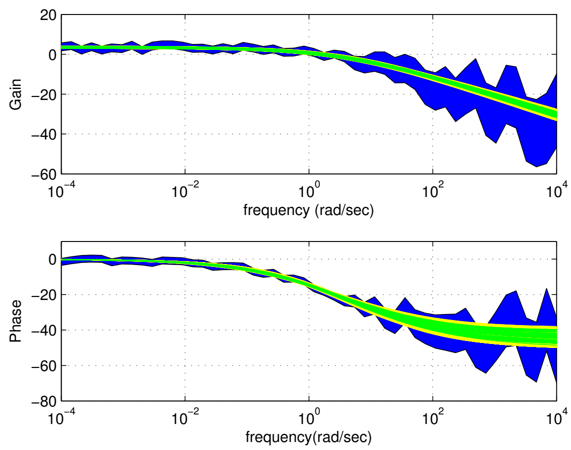

Fig. 9. Gain and phase diagrams of inner (dark) and outer (light) solution sets obtained by applying SIVIA on gain and phase data.

5. CONCLUSION

In this paper, set membership estimation methods have been applied to compute all feasible parameter sets of a fractional differentiation model. First of all, a contractor named *forward-backward propagation* is applied to reduce initial searching space. Then, a set inversion algorithm, *SIVIA*, is applied on gain and phase data. As a result, all parameters, including differentiation order, are expressed as intervals. Furthermore, one of the interesting points of this study is to show the separate contribution of gain and phase data on the final models.

REFERENCES

J. Antoni and J. Schoukens. A comprehensive study of the bias and variance of frequency-response-function measurements: optimal window selection and overlapping strategies. *Automatica*, 43(10):1723–1736, 2007.

J.-L. Battaglia, O. Cois, L. Puigsegur, and A. Oustaloup. Solving an inverse heat conduction problem using a non-integer identified model. *Int. J. of Heat and Mass Transfer*, 44(14):2671–2680, 2001.

W.-C. Chen. Nonlinear dynamics and chaos in a fractional-order financial system. *Chaos, Solitons and Fractals*, 36 (5):1305–1314, 2008.

L. Jaulin and E. Walter. Set inversion via interval analysis for nonlinear bounded-error estimation. *Automatica*, 29 (4):1053–1064, 1993.

L. Jaulin, M. Kieffer, O. Didrit, and E. Walter. *Applied interval analysis.* Springer-Verlag, London, 2001.

P. J. Lawrence and G. J. Rogers. Recursive identification for system models of transfer function type. *Proc. Instn Elec. Engrs.*, 126:283–288, 1979.

L. Le Lay. *Identification fréquentielle et temporelle par modèle non entier.* PhD thesis, Université Bordeaux I, Talence, France, Octobre 1998.

E. C. Levy. Complex curve fitting. *IRE Trans. Autom. Control*, 4:37–43, 1959.

L. Ljung. *System identification – Theory for the user.* Prentice-Hall, 2 edition, 1999.

R. Malti, M. Aoun, J. Sabatier, and A. Oustaloup. Tutorial on system identification using fractional differentiation models. In *SYSID*, pages 606–611, Newcastle, Australia, 29-31 March 2006.

B. Mathieu, A. Oustaloup, and F. Levron. Transfer function parameter estimation by interpolation in the frequency domain. In *EEC'95*, Rome, Italie, 1995.

D. Matignon. Stability properties for generalized fractional differential systems. *ESAIM proceedings - Systèmes Différentiels Fractionnaires - Modèles, Méthodes et Applications*, 5, 1998.

R. E. Moore. *Interval analysis.* Prentice-Hall, Englewood Cliffs, NJ, 1966.

K. B. Oldham and J. Spanier. A general solution of the diffusive equation for semiinfinite geometries. *J. Math. Anal. Appl.*, 39:655–669, 1972.

K. B. Oldham and J. Spanier. Diffusive transport to planar, cylindrical and spherical electrodes. *Electroanaly. Chem. Interfacial Electrochem.*, 41:351–358, 1973.

K. B. Oldham and J. Spanier. *The fractionnal calculus.* Academic Press, New-York and London, 1974.

T. Pritz. Five-parameter fractional derivative model for polymeric damping materials. *Journal of Sound and Vibration*, 265(5):935–952, 2003.

S. Rodrigues, N. Munichandraiah, and A.-K. Shukla. A review of state of charge indication of batteries by means of A.C. impedance measurements. *Journal of Power Sources*, 87:12–20, 2000.

J. Sabatier, M. Aoun, A. Oustaloup, G. Grégoire, F. Ragot, and P. Roy. Fractional system identification for lead acid battery state of charge estimation. *Signal Processing*, 86(10):2645–2657, 2006.

S. G. Samko, A. A. Kilbas, and O. I. Marichev. *Fractional integrals and derivatives: theory and applications.* Gordon and Breach Science, 1993.

C. H. Sanathanan and J. Koerner. Transfer function synthesis as a ratio of two complex polynomilas. *IEEE Trans. Autom. Control*, AC-8:56–58, 1963.

The American Heritage ®. *Dictionary of the English Language.* Houghton Mifflin Company, Boston, 2000.

D. Valério and J. S. da Costa. *Advances in Fractional Calculus Theoretical Developments and Applications in Physics and Engineering*, chapter Identification of fractional models from frequency data, pages 229–242. Springer, 2007.